Research Paper

Topographic effects on the thermal structure of Himalayan glacial lakes: observations and numerical simulation of wind

Kazuhisa A. CHIKITA[a, *]

[a] *Division of Earth and Planetary Sciences, Graduate School of Science, Hokkaido University, Sapporo, 060-0810 Japan*

*Corresponding author. Tel & Fax.: +81-11-706-2764.

E-mail address: chikita@ep.sci.hokudai.ac.jp

Abstract

The thermal structure of two Himalayan glacial lakes, Tsho Rolpa and Imja in the eastern Nepal, was examined by observations in the pre-monsoon seasons of 1996 and 1997. Tsho Rolpa had an isothermal mixed layer at water depths of 0 m to 20 m, whereas Imja did not possess such an isothermal layer. This difference in the thermal structure is explained by the condition that diurnal valley winds, producing wind-driven currents, blow strongly near the water surface of Tsho Rolpa, but very weakly near that of Imja. The wind observations above or near the end moraine indicated that a daily wind system of strong, diurnal valley winds and weak, nocturnal mountain winds is common to the lakes. It was suggested that with respect to the valley winds, the weak winds near the surface of Imja result from topographic screening effects of the upwind dead-ice zone and end moraine 20 to 25 m higher than the water surface. In order to ascertain the topographic effects, three-dimensional numerical simulation of airflow was carried out by making topographic models of actual size in the calculation domain, corresponding to Tsho Rolpa and Imja and their surrounding topography. The simulation revealed that, when winds blow at constant velocities of 1 to 5 m s^{-1} at 2 m above the points corresponding to the weather stations, the wind velocity at 2 m above the water surface for Imja is 33 to 42 % smaller than for Tsho Rolpa. With increasing heights of the end moraine and dead-ice zone, the wind velocity near the lake surface efficiently decreased by decreasing the lake length from 3.1 or 2.2 km to 1.2 km.

Key words: glacial lakes; Nepal Himalayas; thermal structure; wind-driven currents; calving

1. Introduction

Many Himalayan glacial lakes have been expanding by the glacial retreat, probably due to global warming after the Little Ice Age in the 16th to 18th centuries. For example, the surface area of Tsho Rolpa Glacial Lake in the Nepal Himalayas linearly increased from 0.23 km^2 in 1958 to 1.39 km^2 in 1994 (Sakai et al., 2000; Yamada, 2001). In Nepal, such glacial lakes have produced the GLOF (Glacial Lake Outburst Flood) somewhere by the collapse of the end moraine with one GLOF per three years on average (Yamada, 1996). The calving at the glacier terminus (ice cliff) during the recent lake expansion may result from the instability of the ice cliff, which of the basal part keeps direct contact with lake water heated by solar radiation (Yamada, 1996). However, in order to continue calving over the summer, both a heat transport in the surface layer toward the ice cliff and the output of lake water cooled by the glacier melt are needed. By using a turbidity-temperature profiler and mooring systems of current meters and turbidimeters, Chikita et al. (1999) revealed that a lake-current system in Tsho Rolpa is composed of wind-driven, vertical water circulation and sediment-laden underflows from the input of turbid meltwater at the base of the glacier terminus. It was pointed out that the vertical water circulation simultaneously induces vertical thermal circulation to promote the lake expansion by calving at the glacier terminus.

In this study, differences in thermal and density structures between two Himalayan glacial lakes, Tsho Rolpa and Imja, are explained by differences in the intensity of wind-driven currents and the turbidity of input meltwater. By simulating airflow three-dimensionally around the lakes, it is pointed out that the difference in the intensity of wind-driven currents is caused by a difference in the magnitude of wind velocity near the lake surface affected by the topography around the lakes.

2. Observations

2.1. Study areas and methods

The dynamics of two glacial lakes, Tsho Rolpa (4580 m asl) and Imja (5010 m asl) in the eastern Nepal has been examined in the pre-monsoon season of 1996 and 1997 (Fig. 1) (Chikita et al., 1999, 2000). Tsho Rolpa is dammed up by the end moraine and side moraine, whereas Imja is dammed up by the dead-ice zone at downlake and the side moraine. As the histories of lake expansion by the glacial retreat, Tsho Rolpa has been expanding from near the end moraine since 1950's (Mool, 1995), but Imja started to expand from some 100-m scale ponds around site A (Fig. 1) in 1960's. In order to know the thermal and density structures of the lakes, vertical measurements of water temperature and turbidity were conducted at 0.2 m or 1 m intervals at the observation

sites by using a TTD (Temperature-Turbidity-Depth) profiler (model ATU200-P-64K, Alec Electronics Inc., Japan: accuracies of ±0.04 g/l for turbidity and ±0.05 ℃ for temperature). The water turbidity in ppm was converted into suspended sediment concentration (SSC) in g l^{-1}, using the significant correlation of R^2 = 0.88 to 0.89 between turbidity and SSC. The weather conditions (solar radiation, wind velocity, air pressure, air temperature and relative humidity) were observed at site M at ca. 2 m above the end moraine (Fig. 1). The weather station in Tsho Rolpa is located on the island of dead ice near the end moraine. In Tsho Rolpa, in order to clarify the dynamic behaviors of lake water and thereby the condition of heat transport, a mooring sandbag-buoy system of a current meter with a temperature probe (model ACM-8M, Alec Electronics Inc., Japan: accuracies of ±0.5 cm s^{-1} for horizontal current speed, ±3° for horizontal current direction and ±0.01℃ for temperature), a turbidimeter and temperature data loggers was fixed at each of site G, site A and site H. Topographic surveys around Tsho Rolpa and Imja were performed sporadically with a theodolite, which furnished three-dimensional shapes of the end moraine and dead-ice zone at downlake and their height above the lake surface, and heights of ice cliff and side moraine above the lake surface. The accuracies in height and distance were ±0.02 m and ±0.5 m, respectively.

2.2. Results and discussion

Fig. 2 shows the thermal structure of Tsho Rolpa and Imja, longitudinally obtained on 5 June 1996 and 15 July 1997, respectively. Water temperature ranges from 2.3 to 8.5 ℃ in the two lakes. If the water is clear, the water density under pressure applied at each depth ranges from 999.82 kg m^{-3} (8.5 ℃) at the surface of Imja to 1000.58 kg/m^3 (2.3 ℃) at the bottom of Tsho Rolpa. The lakes are thus weakly stratified due to thermobaric effects (e.g. Crwaford and Collier, 1997, Wüest et al., 2005). The seasonal thermocline in Tsho Rolpa is located at 20 to 25 m in depth with water temperature of 3 to 4 ℃, whereas that in Imja is situated near the lake surface with 6 to 8 ℃ (see Yamada, 1996 for seasonal variations in thermal conditions). The thermocline in the lakes tends to thicken gradually toward the glacier terminus (ice cliff). In Tsho Rolpa, a wind-mixed, isothermal layer is developed toward the ice cliff. These suggest that the setup by wind or wind-driven currents prevail in Tsho Rolpa but are very weak in Imja. Being common to the lakes, cold water of 2 to 3 ℃ stays in the lower layer. This is explained by glacier-melt water input from the base of the ice cliff in direct contact at uplake (Chikita et al., 1999). The meltwater into Tsho Rolpa contains suspended matter of mostly silt and clay, but that into Imja is clean (Fig. 3). The density stratification is thus relatively well developed in Tsho Rolpa, especially in the lower layer, because the

meltwater into Tsho Rolpa intrudes into the lower layer as sediment-laden underflow. The bulk density, ρ_{TC} (kg m^{-3}), of lake water at 1 atm is then given by $\rho_{TC} = (1- C / \rho_s) \times \rho_T + C$ as a function of temperature, T (℃) and suspended sediment concentration, C (g l^{-1}), where ρ_T is the water density at T and ρ_s is the particle density (= 2730 kg m^{-3} for Tsho Rolpa and 2750 kg m^{-3} for Imja) of suspended matter. The sediment-laden underflow occurs due to suspended sediment density effects from incoming turbid river water, which has been observed in a reservoir by Chikita (1989) and in a glacier-fed lake by Chikita et al. (1996). Dissolved solids D (g l^{-1}) in lake water were almost uniform at ca. 0.030 g l^{-1} for Tsho Rolpa and at ca. 0.017 g l^{-1} for Imja by chemical analyses. Water pressure P (bar) (P = 0 at the water surface) at each depth was calculated by taking into account water temperature, suspended sediment concentration and dissolved solids. The water bulk density ρ_{TCDP} at pressures and suspended sediment concentration applied were then calculated by the formulas of Chen and Millero (1977) and $\rho_{TCDP} = (1- C / \rho_s) \times \rho_{TDP} + C$.

Fig. 3 shows vertical distributions of water temperature, suspended sediment concentration (SSC), residual density, σ, a square of Brunt-Väisälä Frequency, N, and the temperature, T_{MD}, of the maximum water density at site MD of Tsho Rolpa and Imja. The residual density, σ, is defined by $\sigma = (\rho_{TCDP} - 1000) \times 10$. The Brunt-Väisälä

Frequency, N (= $\sqrt{(g/\rho)(d\rho/dz)}$), is a parameter of the stability in density stratification, where g is the gravitational acceleration, z is the water depth from the lake surface and ρ is the bulk density of water, here corresponding to ρ_{TCD}. The N^2 curves were obtained as 2-m moving averages. The suspended sediment concentration ranges from 0.08 g l^{-1} at the surface to 0.89 g l^{-1} at the bottom. The N^2 distribution in Tsho Rolpa, however, indicates pycnally neutral conditions because of almost zero N^2 throughout depths. The decrease of σ at 77 m depth probably results from the gravitational settling of suspended matter. The isothermal surface layer at depths of less than 14 m corresponds to a wind-mixed layer produced by the strong valley wind (Fig. 4). Imja has the strongest density stability only at the surface with the maximum N^2, due to the highest water temperature. This indicates that a wind near the lake surface is too weak to build up a wind-mixed, isothermal layer. At more than 3 m in depth, Imja has no stability with almost zero N^2. The σ slope is smaller than in Tsho Rolpa, which results from the relatively small suspended sediment concentration of 0.07 to 0.10 g l^{-1}. The suspended sediment concentration (SSC) in Imja is nearly uniform, and the lower layer exhibits relatively low water temperature at depths of more than 73 m. This suggests the meltwater input of SSC similar to or a little more than that of the lake water.

The temperature T_{MD} (℃) giving the maximum water density was calculated by using water pressure and dissolved solids (Chen and Millero, 1977). The intersections at 17.6 m depth in Tsho Rolpa and at 6.2 m depth in Imja indicate the intrusion and stagnation of relatively heavy cold water, here turbid meltwater at depths below the intersections.

The Wedderburn number, $W = (g'h_1 / U_*^2)(h_1 / L)$ was used to judge if or not the setup by wind and vertical water circulation could prevail in Tsho Rolpa and Imja (Stevens and Lawrence, 1997), where h_1 is the water depth of the surface layer interface, L is the lake length in the wind direction, g' is the reduced gravitational acceleration $(= g(\rho_2 - \rho_1)/\rho_1)$, and U_* is the friction velocity for the wind stress, $\tau = \rho_a U_*^2$ (ρ_a: air density). ρ_1 and ρ_2 is the lake water density of the upper and lower layers, respectively. If W is much larger than one, then the setup and upwelling due to wind forcing could not occur, whereas, if W is much smaller than one, then the setup and upwelling is very likely to occur.

Here, the friction velocity U_* at W =1 and the corresponding wind velocity U_2 at 2 m above the lake surface were calculated. The water depth of the thermocline was taken as a boundary between the upper and lower layers of each lake. The depth, h_1, of the surface layer interface was judged to be at 24.2 m depth for Tsho Rolpa and at 4.5 m

depth for Imja (Fig. 3). The mean bulk density, ρ_1, of the upper layer was calculated at 1000.053 kg m^{-3} for Tsho Rolpa and 999.996 kg m^{-3} for Imja, and the mean bulk density, ρ_2, of the lower layer was given at 1000.223 kg m^{-3} for Tsho Rolpa and 1000.038 kg m^{-3} for Imja. The friction velocity $U_* = 0.0177$ m s^{-1} at $W = 1.0$ was thus calculated for Tsho Rolpa from h_1 =24.2 m, L = 3100 m and g' = 0.00166 m s^{-2} (Fig. 2). For Imja, U_* = 0.00263 m s^{-1} at W = 1.0 was obtained from h_1 =4.5 m, L = 1200 m and g' = 0.00041 m s^{-2}. Hence, using the wind stress, $\tau = \rho_a U_*^2 = \rho_a C_d U_2^2$, at the lake surface (air density ρ_a= 0.75 kg m^{-3} at the altitude of 4580 to 5000 m asl and drag coefficient C_d = 0.001 for $U_2 < \sim$1 m s^{-1} (Charnock, 1955; Hsu, 1986), the wind velocity, U_2, at W = 1.0 is 0.56 m s^{-1} and 0.08 m s^{-1} for Tsho Rolpa and Imja, respectively. A condition of W <1 is thus given at $U_2 > \sim$0.6 m s^{-1} for Tsho Rolpa and at $U_2 > \sim$0.1 m s^{-1} for Imja. If U_2 = 5.0 m s^{-1} and 3.0 m s^{-1} over the water surfaces of Tsho Rolpa and Imja, respectively, then W = 0.0087 and 0.00064 for Tsho Rolpa and Imja, respectively. The condition of W much smaller than one implies that the winds can anytime produce the setup and vertical water circulation in the upper layer, due to the wind forcing.

Fig. 4 shows temporal variations of wind vectors (leeward) (a) at 2 m above the lake surface (Tsho Rolpa) near the end moraine and (b) at 2 m above the end moraine (Imja) (see Fig. 1 for location). The daily cycles of strong, diurnal valley winds of 3 to 8

m s^{-1} and weak, nocturnal mountain winds of 0 to 2 m s^{-1} are common to the lakes. Most of the winds blow longitudinally along the lakes. The wind velocity U_2 along Tsho Rolpa ranges from 5 to 8 m s^{-1}on daytime. This means the development of the setup and vertical water circulation in the upper layer of Tsho Rolpa during the valley winds as shown in Figure 2. For Imja, the setup and vertical circulation could occur at wind velocity more than 0.4 m s^{-1}, because then $W <= 0.05$. The weak setup and vertical circulation seem to have occurred in the surface layer of Imja during the observation, since the thermocline gradually thickened toward the ice cliff, suggesting the wind mixing (Fig. 2). The heat transport by wind–driven currents toward the ice cliff and the return flow of water cooled by ice melt at the underwater part of the ice cliff were probably built up in both the lakes, while the strong valley winds blow diurnally (Chikita et al., 1999).

The topographic survey around the lakes indicated that the end moraine and dead-ice zone of Imja are 20 to 25 m higher than the water surface and the end moraine of Tsho Rolpa is 0 to 2 m higher than the surface. In Imja, the tops of the ice cliff and side moraine were 25 m and 70 m higher than the lake surface, respectively. The wind-mixed layer is not developed enough in Imja, since the thermocline is situated near the water surface with 6 to 8 ℃ (Figs. 2 and 3). These suggest that, for the valley

winds, the end moraine and dead-ice zone upwind of Imja produce a topographic screening effect of decreasing the wind velocity near the water surface. Such a decrease in the wind velocity can weak the setup and vertical circulation as in Imja. The wind field inhomogeneity over a lake made up by the surrounding topography directly impacts the hydrodynamics (Endoh et al., 1995, Laval et al., 2003, Rubbert and Köngeter, 2005).

3. Numerical simulation of airflow

3.1. Preparation

In order to ascertain the topographic screening effect of the end moraine and dead-ice zone in Imja Lake, numerical simulation of airflow was carried out. By referring to data of topographic surveys around Tsho Rolpa and Imja and 1/50000 scale topographic maps of 1996 and 1997, topographic models of actual size and shape were built up in the calculation domain of $x \times y \times z$ =7000m×2000m×400m (Fig. 5). The height, H_e, of end moraine and the height, H_i, of ice cliff above the lake surface were given at 1 m and 35 m for Tsho Rolpa, respectively. For Imja, H_i = 25 m, and the height of the end moraine to the dead-ice zone was set as H_e (= 25 m). The height of the side

moraine above the lake surface was commonly given at a constant of 70 m. The geometry of the lake surfaces was taken as rectangles 3100 m long and 400 m wide for Tsho Rolpa and 1200 m long and 400 m wide for Imja. Vertical airflow velocity $w = 0$ and the roughness length z_0 ～0 (smooth boundary) were given as boundary conditions at the lake surface. Considering the atmospheric conditions at the high altitude (Chikita et al., 1999, 2000), the air density $\rho_a = 0.75$ kg m^{-3} and the standard air pressure of 0.6 atm were given for the simulation. Corresponding to the valley-wind velocity observed (Fig. 4), airflow velocity at the inlet (y-z plane at $x = 0$) was given constant at 1.0 to 5.0 m s^{-1} for Tsho Rolpa and at 1.0 to 6.3 m s^{-1} for Imja.

A CFD (computational fluid dynamics) program named "PHOENICS ver. 3.5", which was developed by CHAM, Inc., UK, was used for the simulation (URL: www.cham.co.uk/phoenics/d_polis/d_docs/tr001/tr001.htm). In the program, the completely implicit and hybrid methods were used to resolve discrete types of integral equations of continuity and motion (Navier-Stokes) for incompressible fluids. The eddy viscosity in the Navier-Stokes equation was calculated by using a revised κ - ε model (MMK model) developed by Murakami et al. (1993), Mochida et al. (1993) and Kondo et al, (1995), where κ is the turbulence kinetic energy and ε is the turbulence dissipation rate. Using the MMK model, Tsuchiya et al. (1997) reasonably reproduced

the flow and pressure fields around three types of bluff bodies. The basic grid number in the present simulation is $x \times y \times z = 80 \times 80 \times 80$, and the grid size near the ground and lake surface was set to be relatively small. The airflow velocity and pressure fields under steady state were repeatedly calculated until their values were converged into constants.

In order to examine a difference in the wind-screening effect between the end moraine of Tsho Rolpa and the end moraine to dead-ice zone of Imja, the numerical simulation was similarly performed by changing the height, H_e, at 0 to 55 m on condition of H_i = 35 m and 25 m (const.) for Tsho Rolpa and Imja, respectively. Considering the possibility of lake expansion in the future, some calculations were carried out for Imja 2200 m or 3100 m long. In addition, a barrier's effect of the leeward ice cliff on the wind velocity near the lake surface was inspected by changing the height, H_i, of the ice cliff at 0 to 55m on conditions of H_e = 1 m and 25 m (const.) for Tsho Rolpa and Imja, respectively. After each calculation, the velocity ratio $\alpha = \overline{U_2} / U_e$ was obtained, where U_e is the horizontal flow velocity at 2 m above the end moraine (points of the black circles in Fig. 5).

3.2. Calculated results

Fig. 6 shows spatial distributions of horizontal flow velocity, U_2, at 2 m above the lake surface for Tsho Tolpa (H_e=1 m and H_i =35 m) and Imja (H_e=H_i=25 m). In order that the same velocity of 5.06 m s^{-1} (near the maximum velocity observed) is obtained at the points (black circles in Fig. 4) corresponding to the sites of weather stations (Fig. 1), the flow velocity at the inlet was then given at 5.0 m s^{-1} for Tsho Rolpa and 4.7 m s^{-1} for Imja. The flow velocity, U_e, at 2 m above the end moraine was then 6.47 m s^{-1} for Tsho Rolpa and 5.06 m s^{-1} (black circle) for Imja. The velocity distribution in Tsho Rolpa is affected by both the end moraine and the ice cliff, especially by the ice cliff, showing a decrease of U_2 in the downwind direction within ca. 800 m upwind of the ice cliff. The U_2 in Imja decreases by the end moraine (and dead-ice zone) and ice cliff within ca. 100 m and 200 m, respectively. The end moraine (and dead-ice zone) and ice cliff thus can produce a topographic screening effect and a topographic barrier effect, respectively. The average flow velocity $\overline{U}_2$ over the lake area was then 5.10 m s^{-1} for Tsho Rolpa and 2.98 m s^{-1} for Imja. The flow velocity for Imja is thus 42 % smaller than that for Tsho Rolpa (depletion rate of 0.42). The average wind shear stress, τ_b, at the water surface is given by $\tau_b = \rho_a C_d \overline{U_2}^2$. The average shear stress imposed on the surface of Imja is thus ca. 66 % smaller than for Tsho Rolpa, since the drag coefficient C_d is given

at 0.0012 to 0.0015 for wind velocity of 1 to 6 m s^{-1} (Charnock, 1955; Hsu, 1986). The depletion rate in flow velocity was 0.33 for 1.07 m s^{-1} calculated at the points corresponding to the weather stations. The decrease in depletion rate is thus small for the flow velocity of 1 to 5 m s^{-1} at the points corresponding to the weather stations. Hence, the weak mixing or vertical water circulation in the surface layer of Imja probably results from the wind shear stress being not enough to develop wind-driven currents (Fig. 2).

Fig. 7 shows relations between the velocity ratio, α, the end moraine's height, H_e, and the ice-cliff's height, H_i, above the lake surface. For Imja (L=1200 m), the velocity ratio α decreases linearly with increasing H_e with the good correlation of R^2 = 0.8885, while, for Tsho Rolpa, α decreases rapidly at H_e = 0 to 8 m, but declines gradually at H_e > 8 m (Fig. 7a). Hence, it is suggested that, for glacial lakes dammed up by the relatively long dead-ice zone, the screening effect on the wind velocity over the lake surface is more effective than for glacial lakes dammed up directly by the end moraine. The screening effect of end moraine may be seasonally sensitive in Tsho Rolpa, since the lake level fluctuates at a range of $\pm$ 0.6 m in May to October with no ice cover (Yamada, 1996), thus being H_e < 8 m. The three-dimensional topographic shape of the end moraine (and dead-ice zone), damming up glacial lakes, and a change in the relative

height due to the fluctuation in lake level is thus important to know if or not wind-driven water (and thermal) circulation prevails in the lakes. The velocity ratio α in Imja tends to decline gradually at the lengths of 2200 m and 3100 m. The basin expansion of Imja Lake may thus weaken the screening effect of the dead-ice zone and end moraine.

The barrier's effect of the ice cliff is marked for Imja 1200m long at H_i = 5 to 25 m, but nearly constant at H_i = 25 to 55 m (Fig. 7b). This tendency seems to be unchangeable for the lake expansion up to the lengths of 2200 m and 3100m, though the velocity ratio α wholly increases with increasing lake length. The ice cliff of Tsho Rolpa tends to give nearly constant α at 0.72 to 0.79 for H_{ic} = 0 to 45 m (Fig. 7b). The three-dimensional geometry of the end moraine (and dead-ice zone) could thus affect the efficiency in the barrier's effect of ice cliff.

Any changes in the height of the side moraine and/or the width of the end moraine did not change significantly spatial distributions of the horizontal airflow velocity at 2 m above the lake surface. The existence of the dead-ice zone upwind of glacial lakes and the increase in the height above the lake surface lead to efficiently decrease the wind velocity near the lake surface and control the thermal structure within the lakes.

4. Conclusions

The observations in two Himalayan glacial lakes, Tsho Rolpa and Imja in the pre-monsoon season indicated that the thermal structure is quite different between the two lakes. The existence of the thermocline near the water surface in Imja suggests that the wind velocity near the lake surface is weak at any time. In Tsho Rolpa, the wind-driven, vertical water circulation prevailed with a wind-mixed, isothermal layer. The wind observations above the end moraine indicated a similar wind system between the lakes. The end moraine and dead-ice zone upwind of Imja for the valley winds were 20 to 25 m higher than the lake surface, whereas the end moraine of Tsho Rolpa was only 0 to 2 m higher than the water surface. Hence, the end moraine and dead-ice zone of Imja may produce a topographic screening effect on the wind velocity near the lake surface. The numerical simulation of airflow, using the topographic models of actual size, revealed that the wind velocity at 2 m above the water surface for Imja is 33 to 42 % smaller than for Tsho Rolpa. The 3D topography of end moraine (and dead-ice zone) may have different screening effects of end moraine and different barrier effects of ice cliff on the wind velocity near the lake surface, and thus different thermal structure between Himalayan glacial lakes.

The thermal numerical simulation of lake currents is needed to estimate what

calving rate at the glacier terminus the wind-driven, vertical water circulation could produce.

Acknowledgements

I am indebted to Dr. Tomomi Yamada, Hokkaido Institute of Technology, Japan, for consistent encouragement and invaluable advice to my Himalayan studies. The support team of CHAM-Japan, Inc., gave me helpful advice to get reasonable calculated results. Part of the field observations was conducted in the Research Project of the Cryosphere Research Expedition of Himalaya (CREH) (Supervisor, Prof. Y. Ageta, Nagoya University) in 1994–1999. This study was funded by the Japan International Cooperation Agency (JICA) in 1996 and by the Sumitomo Foundation in 2004-2005. Two reviewers, Dr. Craig Stevens, NIWA, New Zealand and Dr. Bertram Boehrer, UFZ, Germany gave constructive criticisms to this manuscript.

References

Charnock, H., 1955. Wind stress on a water surface. Quarterly Journal of the Royal Meteorological Society 81, 639-640.

Chikita, K., 1989. A field study on turbidity currents initiated from spring runoffs. Water

Resources Research 25, 257-271.

Chikita, K. A., Smith, N. D., Yonemitsu, N. and Perez-Arlucea, M., 1996. Dynamics of sediment-laden underflows passing over a subaqueous sill: glacier-fed Peyto Lake, Alberta, Canada. Sedimentology, 43, 865-875.

Chikita, K., Jha, J. and Yamada, T., 1999. Hydrodynamics of a supraglacial lake and its effect on the basin expansion: Tsho Rolpa, Rolwaling Valley, Nepal Himalaya. Arctic, Antarctic and Alpine Research 31, 58-70.

Chikita, K., Joshi, S.P., Jha, J. and Hasegawa, H., 2000. Hydrological and thermal regimes in a supraglacial lake: Imja, Khumbu, Nepal Himalaya. Hydrological Sciences Journal 45, 507-521.

Crawford, G. B. and Collier, R. W., 1997. Observations of a deep-mixing event in Crater Lake, Oregon. Limnology and Oceanography 42, 299-306.

Endoh, S., Watanabe, M., Nagata, H., Maruo, F., Kawae, T., Iguchi, C. and Okumura, Y., 1995. Wind fields over Lake Biwa and their effect on water circulation. Japanese Journal of Limnology 56, 269-278.

Hsu, S.A., 1986. A mechanism for the increase of wind stress (drag) coefficient with wind speed over water surfaces: a parametric model. Journal of Physical Oceanography 16, 144-150.

Kondo, K., Murakami, S., Mochida, A. and Ishida, Y., 1995. Numerical prediction of flow filed around 2D square rib using revised κ - ε model. Journal of Wind Engineering 63, 35-39.

Laval, B., Imberger, J., Hodges, B. R. and Stocker, R., 2003. Modeling circulation in lakes: Spatial and temporal variations. Limnology and Oceanography 48, 983-994.

Mochida, A. and Ishida, Y. and Murakami, S., 1993. Numerical study on flow field around structures with oblique wind angle based on composite grid system. Proceedings of 7th U. S. National Conference on Wind Engineering, pp. 15-16.

Mool, K.P., 1995. Glacier lake outburst flood in Nepal. Journal of Nepal Geological Society 11, 273-280.

Murakami, S., Mochida, A. and Ooka, R., 1993. Numerical simulation of flow field over surface-mounted cube with various second-moment closure models. Proceedings of 9th Symposium on Turbulent Shear Flow, pp. 13-5-1-13-5-6.

Rubbert, S. and Köngeter, J., 2005. Measurements and three-dimensional simulation of flow in a shallow reservoir subject to small-scale wind field inhomogeneities induced by sheltering. Aquatic Sciences 67, 104-121.

Sakai, A., Chikita, K. and Yamada, T., 2000: Expansion of a moraine-dammed glacial lake, Tsho Rolpa, in Rolwaling Himal, Nepal Himalaya. Limnology and

Oceanography 45, 1401-1408.

Stevens, C.L. and Lawrence, G.A., 1997. Estimation of wind-forced internal seiche amplitudes in lakes and reservoirs, with data from British Columbia, Canada. Aquatic Sciences 50, 115-134.

Tsuchiya, M., Murakami, S., Mochida, A., Kondo, K. and Ishida Y., 1997. Development of a new κ - ε model for flow and pressure fields around buff body. Journal of Wind Engineering and Industrial Aerodynamics 67-68, 169-182.

Wüest, W., Ravens, T. M., Granin, N. G., Kocsis, O., Schurter, M. and Sturm, M., 2005. Cold intrusions in Lake Baikal: direct observational evidence for deep-water renewal. Limnology and Oceanography 50, 184-196.

Yamada, T., 1996. Report on the investigations of Tsho Rolpa Glacier Lake, Rolwaling Valley. Report to Water and Energy Commission Secretariat (WECS), Nepal and Japan International Cooperation Agency (JICA), 129 pp.

Yamada, T., 2001. Meteorological-hydrological environment and thermal regime of a moraine-dammed glacier lake, and their contribution to the lake expansion. Journal of the Japanese Society of Snow and Ice, 63: 223-234.

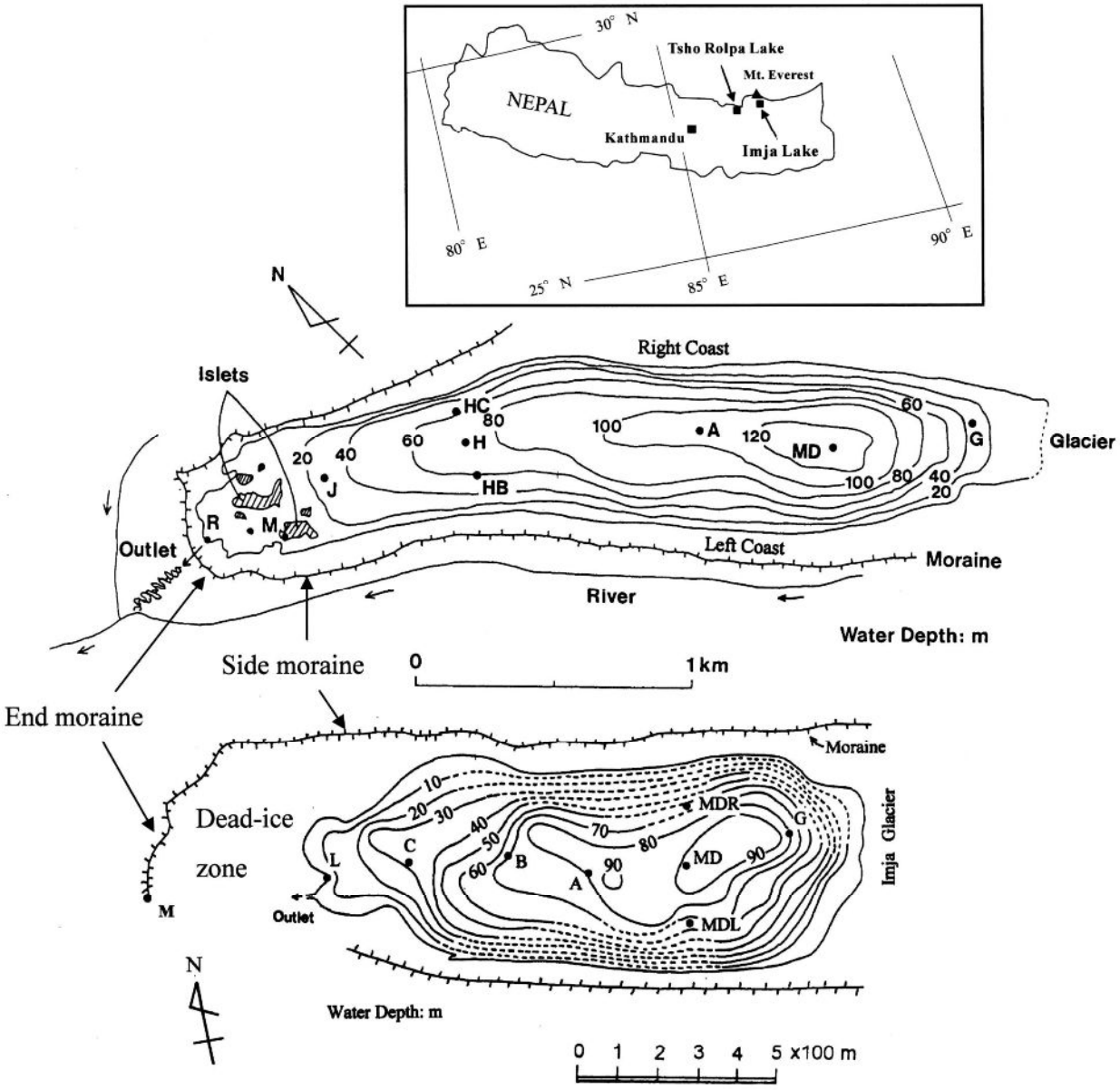

Fig. 1. Location of Tsho Rolpa (upper) and Imja (lower) glacial lakes in Nepal, and observation sites in the lakes on bathymetric maps. Weather stations are located at site M.

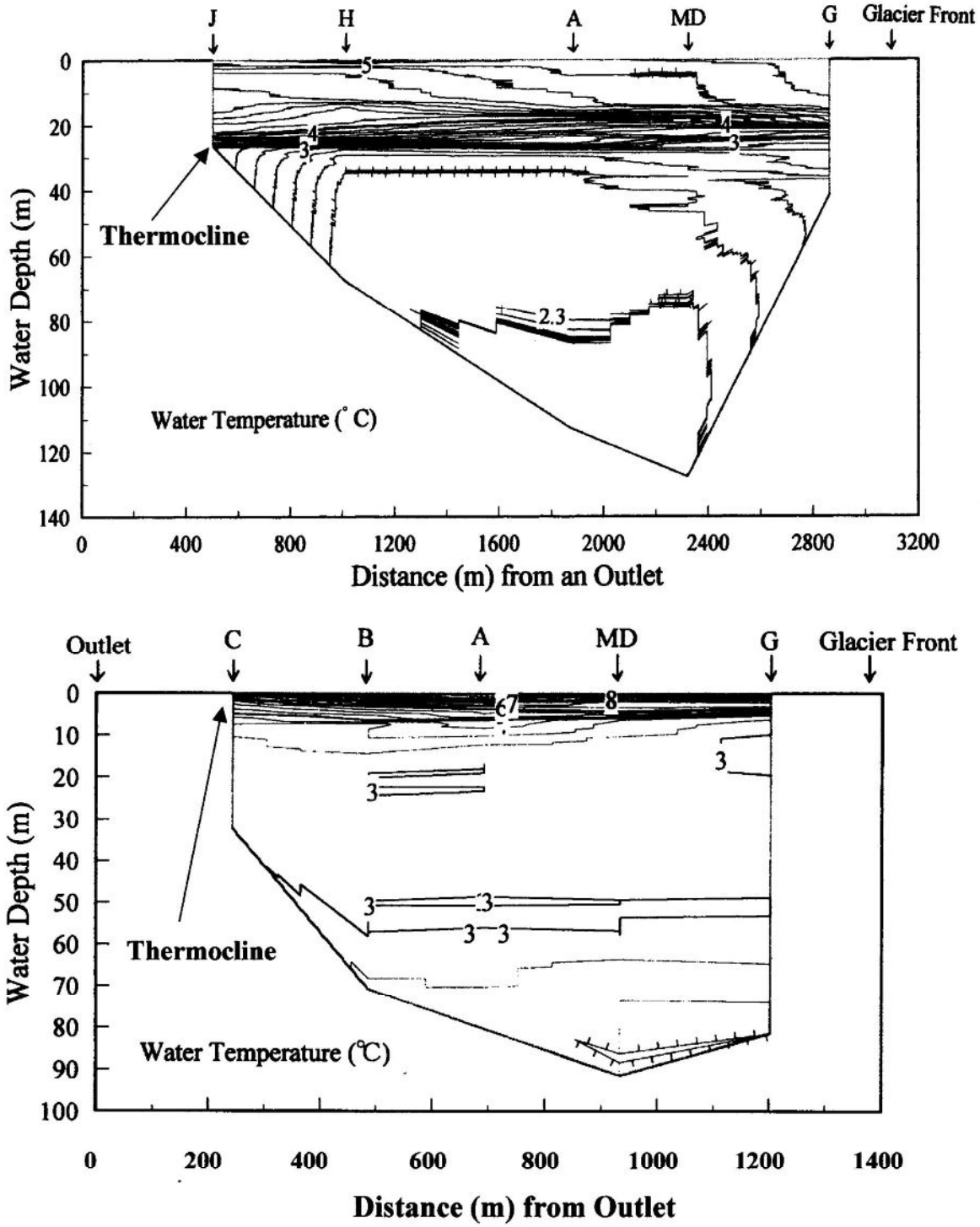

Fig. 2. Longitudinal distributions of water temperature in Tsho Rolpa (upper) and Imja (lower), observed on 5 June 1996 and 15 July 1997, respectively.

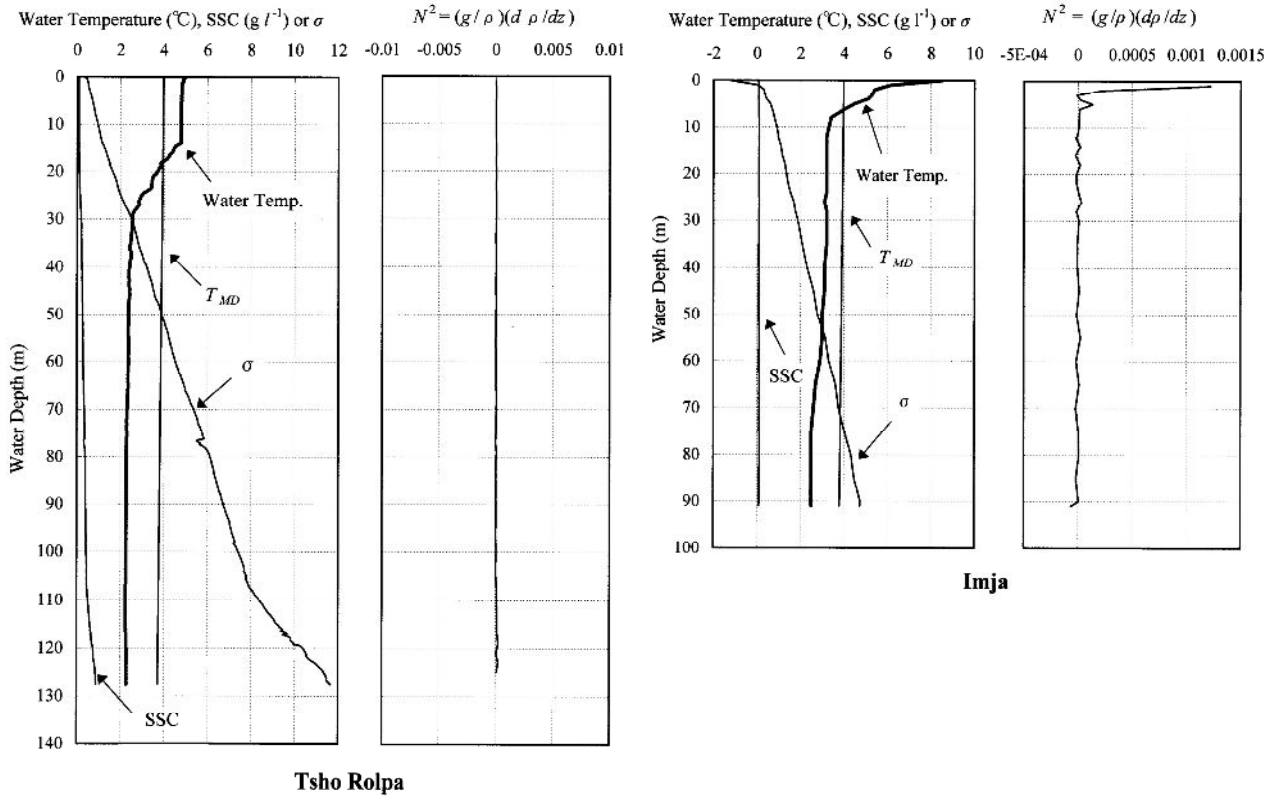

Fig. 3. Vertical distributions of water temperature (℃), suspended sediment concentration (SSC: g l^{-1}), residual density, σ, and a square of Bunt-Väisälä Frequency, *N*, at the deepest points (site MD) of Tsho Rolpa (5 June 1996) and Imja (15 July 1997). T_{MD} is the temperature of the maximum water density at pressure and dissolved solids applied.

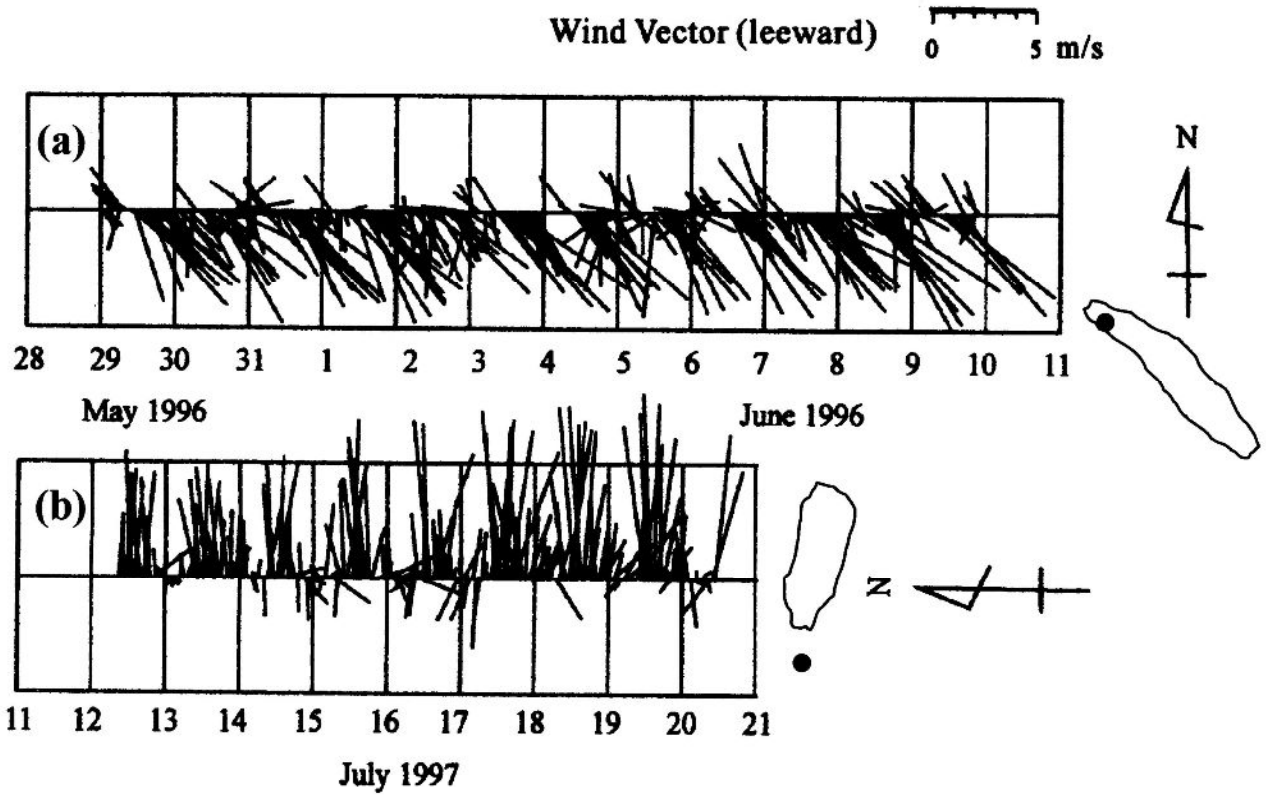

Fig. 4. Time series of wind vectors (leeward) at the weather stations (site M) of (a) Tsho Rolpa and (b) Imja. The location of site M is shown by the black circles with the outlined lakes.

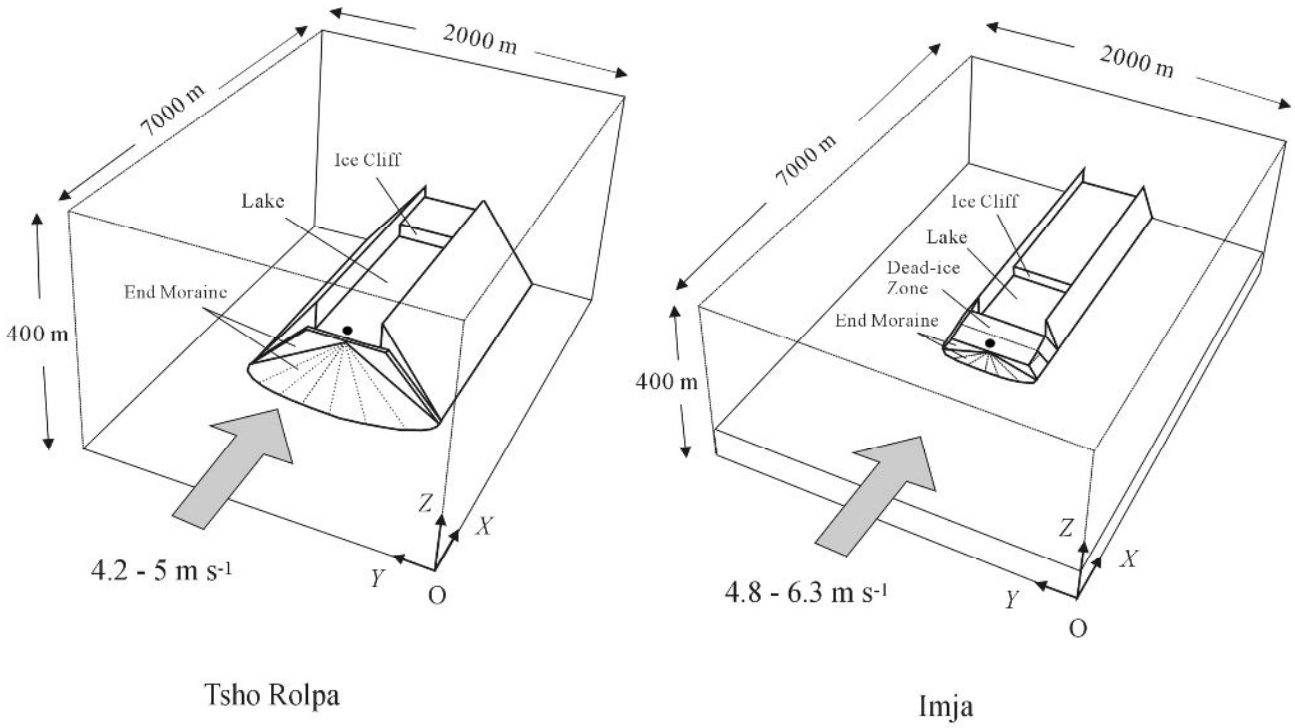

Fig. 5. Topographic models of Tsho Rolpa and Imja made in the calculation domain of airflow simulation. The three dimensional shapes around rectangular lakes are followed by the topographic surveys and 1/50000 scale topographic maps. The airflow velocity at 2 m above the top of the end moraine (black circles) was compared with that at 2 m above the lake surface.

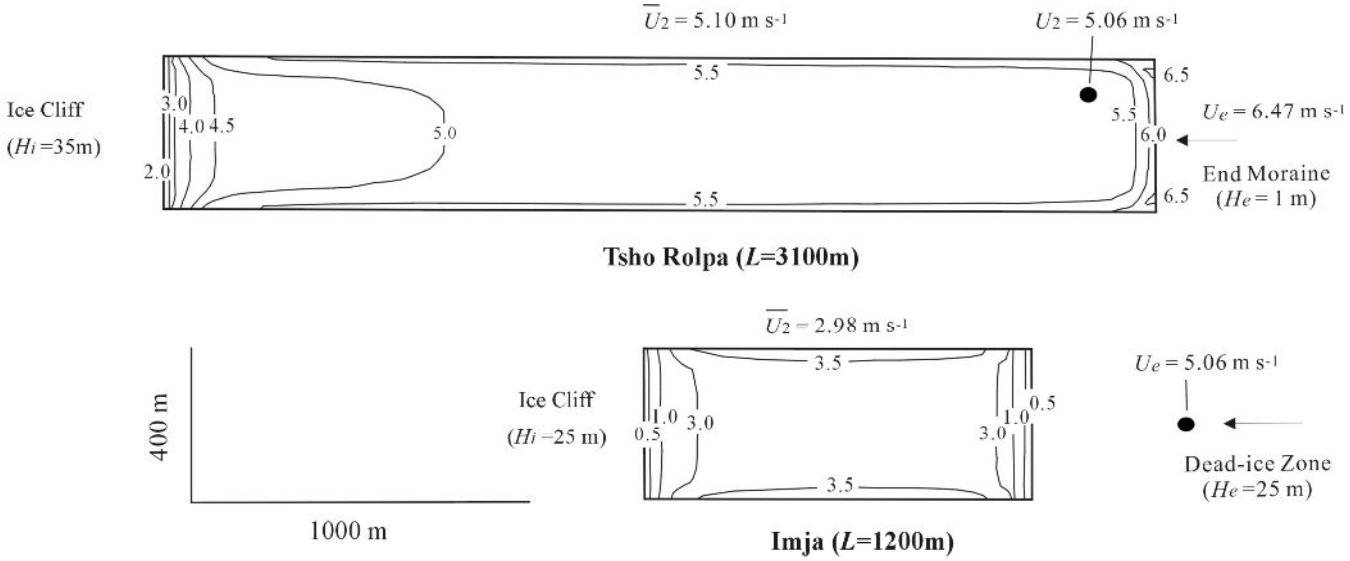

Fig. 6. Spatial distributions of horizontal airflow velocity, U_2 (m s^{-1}), at 2 m above the lake surface calculated for topographic models of Tsho Rolpa (upper) and Imja (lower). The same airflow velocity of 5.06 m s^{-1} was given at the points of black circles, corresponding to the sites (site M) of the weather stations in Figures 1 and 4. The airflow velocity, $\overline{U_2}$, averaged over the lake surface and the air flow velocity, U_e, at 2 m above the end moraine (black circles in Fig. 5) are numerically shown.

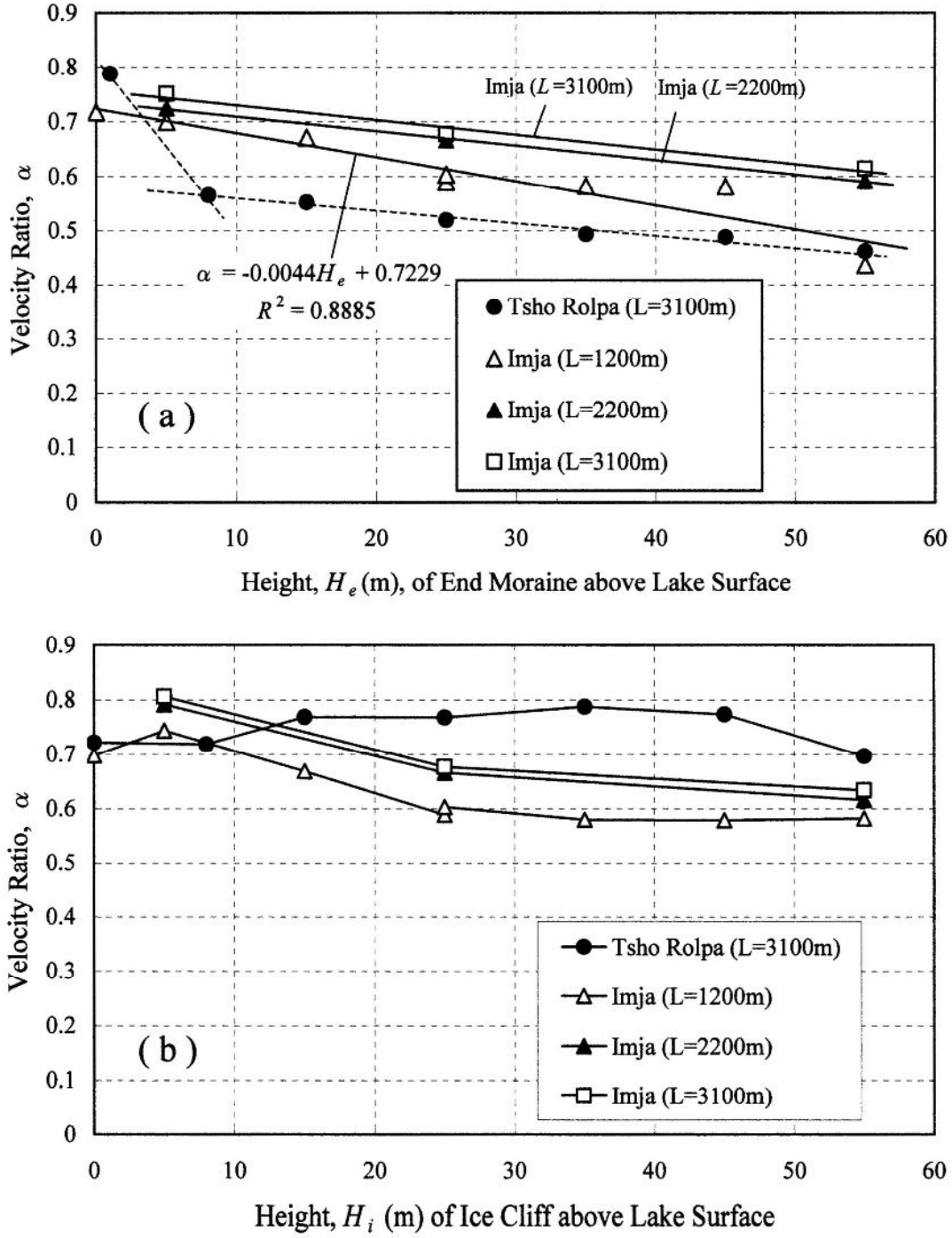

Fig. 7. Relations (a) between the velocity ratio, $\alpha = \overline{U_2}/U_e$ and the height, H_e, of end moraine (and dead-ice zone) and (b) between α and the height, H_i, of ice cliff.